Controlling the red luminescence from silicon quantum dots in hydrogenated amorphous silicon nitride films

H. L. Hao, L. K. Wu, and W. Z. Shen[a)]
Laboratory of Condensed Matter Spectroscopy and Opto-Electronic Physics, Department of Physics, Shanghai Jiao Tong University, 1954 Hua Shan Road, Shanghai 200030, People's Republic of China

(Received 28 January 2008; accepted 6 March 2008; published online 28 March 2008)

We report on a simple way to control the red luminescence from silicon quantum dots (Si QDs) in hydrogenated amorphous silicon nitride. The achievement has been realized through annealing treatments, which effectively modify the dot size, density, and surface chemistry. High resolution transmission electron microscopy, Raman scattering, infrared absorption, and x-ray photoelectron spectroscopy have been employed to reveal the existence, chemical compositions, bonding environment, and evolution of the Si QDs. We have also identified the transition of the dominant luminescence mechanism in the Si QDs from quantum confinement effect to interface state assisted radiative recombination. © *2008 American Institute of Physics*. [DOI: 10.1063/1.2902296]

Low-dimensional silicon (Si) materials have been attracting more and more attention to seek visible luminescence for Si optoelectronic applications. Efficient room-temperature photoluminescence (PL) and/or electroluminescence have been realized in several nanometer-sized Si materials.[1,2] The previous interest was in the light emission from Si nanostructures in silicon oxide films. However, theoretical and experimental studies suggest that there are extremely high potential barriers ($\sim$8.5 eV),[3] which seriously decrease the injection efficiency of carriers. Due to the relatively lower barrier ($\sim$2.0 eV) for carriers and more intense light emission than those of silicon oxide, hydrogenated amorphous silicon nitride (α-SiN$_x$:H) films embedded with Si quantum dots (Si QDs) represent good candidates for the Si-based light-emitting devices. We have recently presented a detailed investigation for the origin of the room-temperature visible luminescence in α-SiN$_x$:H.[4]

It is generally accepted that the quantum confinement effect (QCE) has played a dominant role in the light emission from the Si QDs in α-SiN$_x$:H thin films. Nevertheless, the QCE is not the sole mechanism responsible for the visible PL since most of the reported light emission resulting from Si QDs is limited in the red range.[5,6] Surface/interface state assisted radiative recombination has been assigned in Si QDs,[7,8] and Wang *et al.*[9] have suggested that the surface passivation in terms of introducing localized states in the band gap is also an important factor affecting the light emission. As we know, the structure and surface chemistries determine the nature of the luminescence,[9,10] while annealing treatment is a simple and effective technique to modify the Si QD size, density, and chemical configurations.

The α-SiN$_x$:H films (with thickness of $\sim$350–380 nm) were grown under temperature (T_d) of 300–500 °C by a plasma enhanced chemical vapor deposition system on *p*-type Si substrates. After the deposition, the samples were annealed at temperatures (T_A) of 500–1100 °C for 30 min in argon ambient. PL and Raman scattering spectra were performed on a Jobin Yvon LabRAM HR 800 UV micro-Raman spectrometer using 514.5 nm line of Ar$^+$ laser and 325.0 nm line of He–Cd laser, respectively. The existence and evolution of the Si QDs were revealed by high resolution transmission electron microscopy (HRTEM) (JEOL JEM-2100F) and infrared absorption spectra (from Nicolet Nexus 870 Fourier transform infrared spectrometer). The chemical compositions and bonding environment were analyzed by a PHI Quantum 2000 x-ray photoelectron spectroscopy (XPS).

Figure 1(a) presents the room-temperature PL spectra of the α-SiN$_x$:H thin films. We can clearly observe that there is an obvious redshift from around 1.82 eV in the as-deposited sample to 1.76 eV in the one with T_A=800 °C, accompanied with a strong enhancement of the luminescence intensity by a factor of 15. The PL peak exhibits a continuous redshift from 1.76 to 1.70 eV with the further increase of T_A to 1100 °C, however, the luminescence intensity drastically decreases. Similar PL behaviors from Si QDs have been observed in the silicon oxide films.[2] Furthermore, the luminescence peak displays quite different temperature dependences in the annealed α-SiN$_x$:H thin films. Figures 1(b) and 1(c) show the typical temperature-dependent PL spectra of the thin films (T_d=400 °C). We find that with the increase of the temperature, a significant redshift of the peak occurs in α-SiN$_x$:H annealed below or at 800 °C. In contrast, the PL peak remains almost unchanged under higher T_A. It is reasonable to assume that there are different Si QD-related emission mechanisms responsible for the observed PL bands.

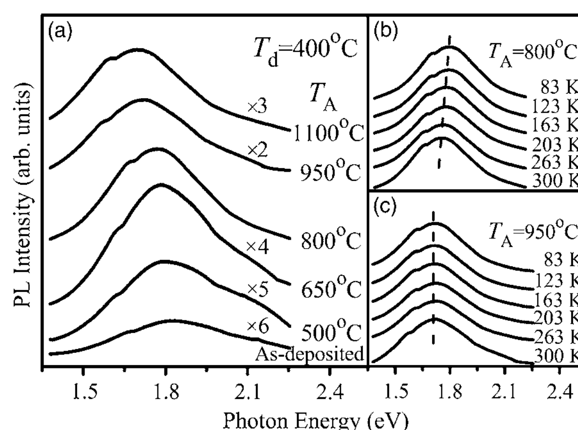

FIG. 1. (a) Room-temperature PL spectra of α-SiN$_x$:H films with T_d=400 °C under different T_A. Temperature-dependent PL spectra of the thin films annealed at (b) 800 °C and (c) 950 °C.

a)Author to whom correspondence should be addressed. Electronic mail: wzshen@sjtu.edu.cn.

0003-6951/2008/92(12)/121922/3/$23.00

© 2008 American Institute of Physics
Author complimentary copy. Redistribution subject to AIP license or copyright, see http://apl.aip.org/apl/copyright.jsp

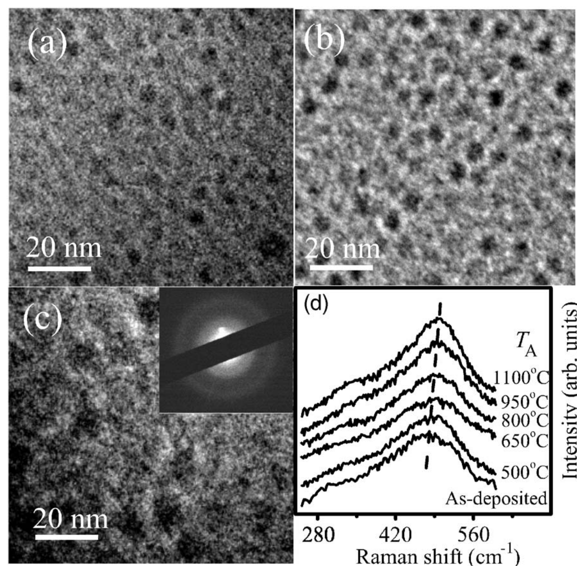

FIG. 2. Cross-sectional HRTEM images of the (a) as-deposited sample and annealed ones at (b) 800 °C, and (c) 1100 °C, together with the transmission electron diffraction pattern from α-Si QDs shown in the inset. (d) Raman spectra of the same samples as in Fig. 1(a).

We start from the HRTEM measurements [Figs. 2(a)–2(c)] for the evolution of the Si QD size and density with T_A. No lattice fringes can be observed, indicating that these Si QDs are amorphous. From the figures, we can clearly observe the change of the amorphous Si (α-Si) QD size. The average dot size increases from around 3.6 nm in the as-deposited sample to ~4.9 nm in the annealed one at 800 °C. These sizes correspond to the red luminescence according to the QCE model for α-Si QDs embedded in α-SiN$_x$:H thin films,[1] while the observed enhancement of the α-Si QD density from 7.6×10^{12} to 1.1×10^{13} cm^{-2} explains the increase of the PL intensity for α-SiN$_x$:H annealed below/at 800 °C in Fig. 1(a).

With the further increase of T_A to 1100 °C, the average dot size in Fig. 2(c) drastically increases to ~9.8 nm with the density of 2.5×10^{12} cm^{-2}; the QCE becomes very weak within such large QDs. In combination with the observation of temperature independent PL peak position in the α-SiN$_x$:H thin films under $T_A>800$ °C, we will assign later that the luminescence is related to the QD/SiN$_x$ interface states for the samples with high T_A. The inset of Fig. 2(c) illustrates the transmission electron diffraction pattern, which exhibits a series of diffused halos, suggesting that the Si QDs are still in amorphous even at such a high T_A.[11] Figure 2(d) displays the Raman spectra of the same samples, as in Fig. 1(a). The Raman peaks fall in the range from ~494 to 499 cm^{-1}, where the position of α-Si QDs always lies.[4] With increasing T_A, the peak shifts toward the higher energy and the linewidth becomes narrower, both of which indicate the increase of α-Si QD size.[3] The increase of Si QD size leads to the enrichment of the Si/SiN$_x$ interface states, which prevents the crystallization of α-Si QDs.[12]

We now turn to the infrared absorption measurements [Fig. 3(a)] for the direct information about the chemical bonds inside α-SiN$_x$:H. The absorption bands at around 605, 820, 1090, 2150, and 3300 cm^{-1} can be assigned to the modes of Si–H bending, asymmetric Si–N stretching, N–H rocking, Si–H stretching, and N–H stretching, respectively.[4] With the increase of T_A, the hydrogen bonds (Si–H and N–H

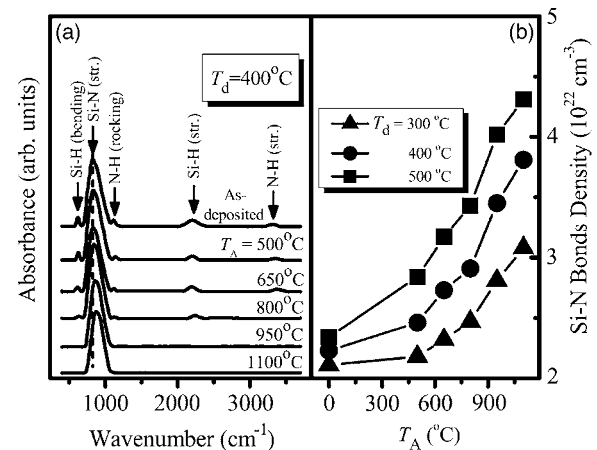

FIG. 3. (a) Room-temperature infrared absorption spectra for the same samples as in Fig. 1(a). (b) Densities of Si–N bonds as a function of T_A for the samples with different T_d.

bonds) gradually decrease and disappear at $T_A=950$ °C, where the hydrogen completely effuses from α-SiN$_x$:H thin films and, therefore, some nonradiative recombination centers such as dangling bonds would not be passivated. This can be well explained by the simple chemical reaction in the annealing process: $\mathrm{Si-H+N-H\rightarrow Si-N+H_2}$. We can also observe that with increasing T_A, the peak position of the asymmetric Si–N stretching mode continuously shifts toward high energy. By integrating the absorption bands, we have calculated the densities of Si–N bonds for the samples with different T_A and T_d, as shown in Fig. 3(b). It is clear that the Si–N bond density increases with T_A for all α-SiN$_x$:H thin films, as expected from the above chemical reaction. The Si–N peak blueshift and density increment both indicate that the number of nitrogen atoms bonded to one Si atom is larger at higher T_A.[6] While the N/Si ratio remains unchanged for the samples with the same T_d, the change of the Si–N peak is expected to be accompanied by the increase of Si phase.[6,13]

Figure 4(a) displays the experimental (open circles) and calculated (solid curves) Si $2p$ core-level binding energy spectra of the α-SiN$_x$:H thin films. We have employed the random bonding model to analyze the bonding configurations of Si-rich silicon nitride thin films, under which the α-SiN$_x$ network is considered as a statistical distribution of the $\mathrm{Si-Si_{4-n}N_n}$ ($n=0$, 1, 2, 3, or 4). With the increasing value

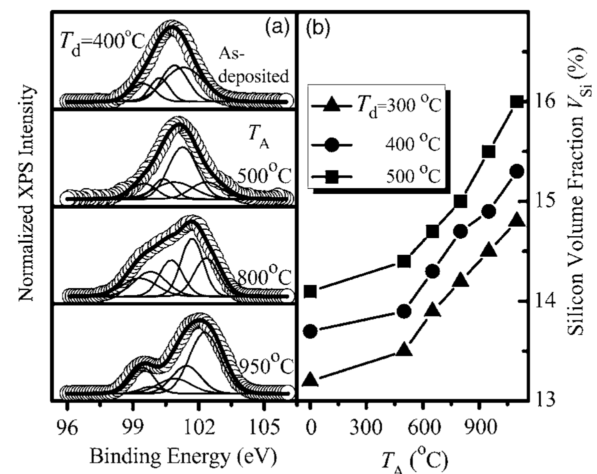

FIG. 4. (a) Si $2p$ XPS spectra for the same samples as in Fig. 1(a). (b) Si volume fractions V_{Si} as a function of annealing temperature T_A for the samples with different deposition temperatures T_d.

Author complimentary copy. Redistribution subject to AIP license or copyright, see http://apl.aip.org/apl/copyright.jsp

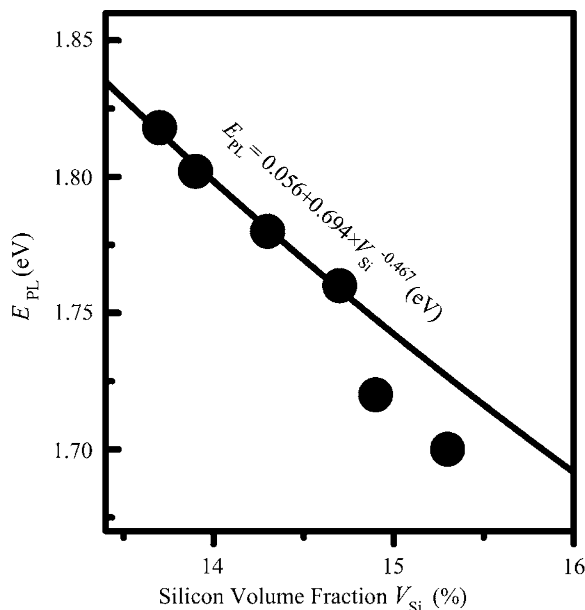

FIG. 5. Relationship between the PL peak energy E_{PL} and V_{Si} in Si QDs. The solid curve is the calculated results through the QCE model.

of n, the peak energy of $Si-Si_{4-n}N_n$ increases from around 99.5 ($n=0$) to 102.5 eV ($n=4$).[6] Since the Si_3N_4 in the as-deposited α-SiN_x:H film would not be generated until the deposition temperature is over 500 °C,[14] the Si_3N_4 phase has been excluded in the fitting for the as-deposited sample.

In the as-deposited thin film, the broad Si 2p peak located around 100.7 eV corresponds to the mixture of subnitride species. After annealing treatments, the main peak shifts toward the high energy and no other noticeable changes are observed in the spectra before T_A reaches 800 °C. At $T_A=800$ °C, the shoulder at low energy side around 99.5 eV can be identified as a characteristic of pure Si phase.[6,13] With further increasing T_A to 950 °C, the peak at 99.5 eV becomes much clearer, and the main peak energy has a progressive shift up to 102.0 eV, close to the stable $Si-N_4$ phase.[5] The XPS results clearly demonstrate that at high T_A (>800 °C), the pure Si and nitrogen-rich phases approximating Si_3N_4 would dominate in Si nitride. Through the integrated intensities of the pure Si and Si 2p peaks, we list in Fig. 4(b) the Si volume fractions (V_{Si}) for the α-SiN_x:H samples deposited at different temperatures. It is clear that V_{Si} progressively increases with T_A at any T_d due to the decomposition of the unstable subnitride phases.

With the increase of T_A, annealing treatments contribute to create new Si QDs and increase the size of already existing Si QDs.[2] On the one hand, by creating new Si–Si bonds between Si atoms previously bonded to hydrogen atoms, the effusion of hydrogen allows the growth of additional Si QDs, which results in the increase of Si QD density. On the other hand, more Si atoms at higher T_A randomly disperse in the annealed films, they tend to nucleate and grow up. The growth rate of Si QDs increases with V_{Si}, leading to the larger Si QDs at higher T_A. However, when T_A increases over 800 °C, the coalescence, overgrowth, and expansion of Si QDs will reduce the dot density but still increase the dot size.

We have examined in Fig. 5 the relationship between the PL peak energy and Si volume fraction for the PL mechanism, where the solid curve is the calculated results through the QCE model: $E_{PL}=P_1+P_2\times V_{Si}^{-P}$. The fitted exponent P is found to be 0.467, which is close to the $d^{-1.39}$ law (with d as the QD radius).[15] It is clear that the relationships of E_{PL} versus V_{Si} for the samples annealed at $T_A \leq 800$ °C agree well with the QCE model, strongly indicating that their PL originates from the Si QDs via QCE. However, there is a very clear offset from the QCE expectation in those under $T_A>800$ °C. As we know, large Si QDs under $T_A>800$ °C result in high interface state density, which makes the associated radiative recombination play a more crucial role, as compared with the QCE in the luminescence.[8,9] Considering the temperature independence of the luminescence peak in Fig. 1(c) and the complete effusion of hydrogen revealed in Fig. 3(a), the possibility of the red PL originating from the hydrogenation of the Si QDs surface can be excluded for the films with T_A over 800 °C. Therefore, we can assign the red PL under $T_A>800$ °C to the electrons trapped at localized states, which are formed by interface states close to the conduction edge in the surface vicinity of Si QDs.[8] The localized levels formed by the interface states are also size dependent: the energy gap of localized states decreases with increasing Si QD size due to the increase of interface states,[16] which results in the observed redshift of the PL peak in Fig. 1(a).

Finally, we discuss the mechanisms for the rapid decrease of the luminescence intensity in α-SiN_x:H under T_A over 800 °C. (i) Due to the effusion of hydrogen, the dangling bonds acting as nonradiative recombination centers cannot be well passivated. (ii) With the decrease of the Si QD density, there are fewer excited electron-hole pairs that can be transferred from the band edge of QDs to the interface related states.[8] (iii) The enhanced Si QD have larger surface areas and surface roughness, as revealed by atomic force microscopy images, which hinder the radiative recombination of carriers and sequentially quench the PL.

This work was supported by the Natural Science Foundation of China under Contract Nos. 10674094 and 10734020, National Major Basic Research Project No. 2006CB921507, National Ministry of Education Program of IRT0524, and Shanghai Project of 06JC14039.

[1]N.-M. Park, C.-J. Choi, T.-Y. Seong, and S.-J. Park, Phys. Rev. Lett. **86**, 1355 (2001).
[2]H. Rinnert, M. Vergnat, G. Marchal, and A. Burneau, Appl. Phys. Lett. **72**, 3157 (1998).
[3]Y. Q. Wang, Y. G. Wang, L. Cao, and Z. X. Cao, Appl. Phys. Lett. **83**, 3474 (2003).
[4]H. L. Hao, L. K. Wu, W. Z. Shen, and H. F. W. Dekkers, Appl. Phys. Lett. **91**, 201922 (2007).
[5]M. H. Wang, D. S. Li, Z. Z. Yuan, D. R. Yang, and D. L. Que, Appl. Phys. Lett. **90**, 131903 (2007).
[6]M. Molinari, H. Rinnert, and M. Vergnat, J. Appl. Phys. **101**, 123532 (2007).
[7]L. D. Negro, J. H. Yi, J. Michel, L. C. Kimerling, T.-W. F. Chang, V. Sukhovatkin, and E. H. Sargent, Appl. Phys. Lett. **88**, 233109 (2006).
[8]Z. H. Cen, J. Xu, Y. S. Liu, W. Li, L. Xu, Z. Y. Ma, X. F. Huang, and K. J. Chen, Appl. Phys. Lett. **89**, 163107 (2006).
[9]X. X. Wang, J. G. Zhang, L. Ding, B. W. Cheng, W. K. Ge, J. Z. Yu, and Q. M. Wang, Phys. Rev. B **72**, 195313 (2005).
[10]K. Ma, J. Y. Feng, and Z. J. Zhang, Nanotechnology **17**, 4650 (2006).
[11]Y.-B. Park and S.-W. Rehee, J. Appl. Phys. **90**, 217 (2001).
[12]M. Zacharias, J. Bläsing, P. Veit, L. Tsybeskov, K. Hirschman, and P. M. Fauchet, Appl. Phys. Lett. **74**, 2614 (1999).
[13]M. H. Wang, D. R. Yang, D. S. Li, Z. Z. Yuan, and D. L. Que, J. Appl. Phys. **101**, 103504 (2007).
[14]J. J. Mei, H. Chen, W. Z. Shen, and H. F. W. Dekkers, J. Appl. Phys. **100**, 073516 (2006).
[15]H. Rinnert, M. Vergnat, and A. Burneau, J. Appl. Phys. **89**, 237 (2000).
[16]G. Hadjisavvas and P. C. Kelires, Phys. Rev. Lett. **93**, 226104 (2004).

Author complimentary copy. Redistribution subject to AIP license or copyright, see http://apl.aip.org/apl/copyright.jsp